  Bull. Chem. Soc. Jpn., 65, 1957—1966 (1992)

Atropisomerism in Doubly *peri*-Substituted 9-(2-Methylbenzyl)triptycene Derivatives, 8-Chloro- and 8-Bromo-1,4-dimethyl-9-(2-methylbenzyl)triptycenes

Gaku YAMAMOTO,* Takashi NEMOTO,† and Yuji OHASHI*,†
Department of Chemistry, Faculty of Science,
The University of Tokyo, Bunkyo-ku, Tokyo 113
† Department of Chemistry, Faculty of Science,
Tokyo Institute of Technology, Meguro-ku, Tokyo 152
(Received March 2, 1992)

The ^{13}C dynamic NMR study revealed that 9-(2-methylbenzyl)triptycene has an energy barrier to gear rotation of 11.8 kcal mol^{-1} (1 cal=4.184 J). Introduction of substituents at two of the *peri*-positions was expected to raise the barrier enough for atropisomerism to be realized in this system. Actually, two stable rotational isomers, *ap* and *sc**(9*S**), were separately isolated for 8-chloro- (**7**) and 8-bromo-1,4-dimethyl-9-(2-methylbenzyl)triptycene (**8**). Classical kinetic studies in toluene-d_8 solutions revealed that the isomerization barriers ($\Delta G^{\ddagger}$ at 350 K) are 26.4 and 27.2 kcal mol^{-1} for **7** and **8**, respectively. Isomerization pathways were investigated by molecular mechanics calculations, which suggested that gear rotational pathway was favored. In either compound, the *sc** (9*S**) rotamer was found to thermally isomerize to the *ap* rotamer in the solid state. X-Ray crystallographic analysis of the rotameric crystals showed that the rotamers had different crystal structures and thus the crystal would be destroyed during the isomerization.

Atropisomerism is defined as stereoisomerism due to restricted rotation about single bonds where the isomers can actually be isolated.[1] In order for rotational isomers to be isolated in solution at 25 °C, the free energy of activation for the internal rotation must be higher than ca. 24 kcal mol^{-1}. This value corresponds to the rate constant of 1.6×10^{-5} s^{-1} and the half-life of ca. 6 h if the equal amounts of two isomers are present at equilibrium. Many examples of atropisomerism have been reported[2] and most of them are for bonds between sp^2-hybridized carbon atoms, typically represented by biphenyls and tetraarylporphyrin derivatives. Studies on atropisomerism involving sp^3-hybridized atoms belong to a rather new and less studied area,[2] and as for sp^3-hybridized C–C bonds only a few examples are known.[2-11]

We reported in 1972 the first example of atropisomerism involving an sp^3-hybridized carbon bond in dimethyl 9-(α,α-dimethylphenethyl)-9,10-dihydro-9,10-ethenoanthracene-11,12-dicarboxylate (**1**), where the *meso* and *dl* isomers due to restricted rotation about the bridgehead-to-substituent bond were separately isolated[3] and the optical resolution of the *dl* isomer was attained.[4] In order to further raise the energy barrier to rotation, the ethenoanthracene skeleton was replaced by the even more rigid triptycene skeleton. Several examples of atropisomerism have been found in 9-substituted triptycene derivatives.[5-9] When the 9-substiuent is a tertiary alkyl group, highly stable atropisomers are isolated even if the triptycene skeleton does not carry substituents at the *peri*-positions.[5,6] When a benzyl group is at the bridgehead, atropisomerism is attained if all of the three *peri*-positions are substituted as in **2**.[12a]

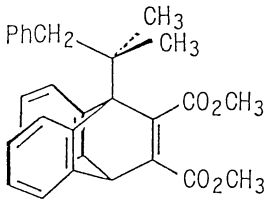

1

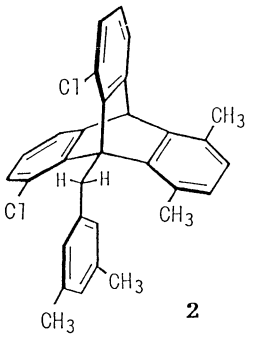

2

Compound **2** has a unique feature that not only the rotation about the triptycene-to-methylene (Tp–CH_2) bond is frozen on the laboratory time scale but also the aryl-to-methylene (Ar–CH_2) bond is restricted on the NMR time scale. The molecule exists in the conformation shown and thus is regarded as a molecular gear composed of a three-toothed wheel (Tp) and a two-toothed wheel (Ar) in a static sense. As easily recognized by inspection of molecular models, rotation about the Tp–CH_2 bond is always accompanied by rotation about the Ar–CH_2 bond. We refer to this process as gear rotation (GR). Rotation about the Ar–CH_2 bond takes place not only concomitantly with the rotation about the Tp–CH_2 bond (GR) but also independently of the Tp–CH_2 rotation, which we refer to as isolated rotation (IR). In the case of **2**, the IR processes have far lower energy barriers (15.5 and 16.6 kcal mol^{-1} at the *ap* and ±*sc* sites, respectively) than the GR process (25.2 kcal mol^{-1} for the *ap*→±*sc* process).[12c]

The energy barriers to these processes should depend on the substitution patterns of the Tp and Ar moieties. We got interested in the design of molecules with GR as the lowest energy process and with a variety of GR barriers ranging from those detected by dynamic NMR

spectroscopy to those manifesting atropisomerism.

The ^{13}C dynamic NMR and molecular mechanics studies on 9-benzyltriptycene (**3**) and 9-phenoxytriptycene (**4**), the simplest molecular gears of the present concern, revealed that in **3** the IR process was shown to have a lower energy barrier than the GR process, while GR is the most favored process in **4**.[13]

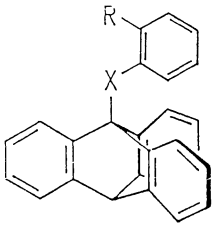

3: X=CH_2, R=H
4: X=O, R=H
5: X=CH_2, R=CH_3
6: X=O, R=CH_3

Introduction of a suitable substituent into an ortho position of the phenyl group in **3** was expected to raise the IR barrier and thus render the GR process more favored, and 9-(2-methylbenzyl)triptycene (**5**) was chosen as a model system. ^1H dynamic NMR study of a series of singly *peri*-substituted 9-(2-methylbenzyl)triptycenes was performed,[14] which revealed an interesting dynamic behavior explained in terms of gear rotation, and showed that the energy barrier separating rotamers was 21 kcal mol^{-1} at the highest, which was still too low for atropisomerism to be attained. Introduction of two *peri*-substituents in **5** seemed promising and 8-chloro-1,4-dimethyl-9-(2-methylbenzyl)triptycene (**7**) and its 8-bromo derivative (**8**) were chosen as target compounds, which was successful as described in detail in this article.[15a]

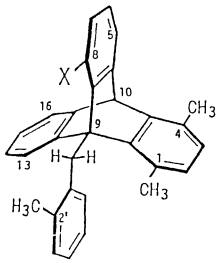

7: X=Cl
8: X=Br

The dynamic behavior of 9-(2-methylbenzyl)triptycene (**5**) itself has escaped investigation because the internal motion of the molecule was reflected only in the lineshapes of the aromatic proton and carbon signals and low-field CW NMR machines could not afford the quantitative information. We now studied the dynamic behavior of **5** and its oxygen analog, 9-(2-methylphenoxy)triptycene (**6**), by ^{13}C dynamic NMR and molecular mechanics calculations. At the outset we describe the results of the study in this line.

Results and Discussion

^{13}C Dynamic NMR Studies on 5 and 6. In both of compounds **5** and **6** the rotation about the Tp–X bond was fast on the NMR time scale at 25 °C rendering three benzene rings of the Tp moiety equivalent. In the ^1H NMR spectrum, lowering of the temperature caused broadening and further splitting of the signals in the aromatic proton region but induced no change in the *o*-methyl and methylene signals even at the lowest temperature of −90 °C. This suggested that the molecules existed in a single conformation with the *o*-methyl group pointing outward.

As quantitative kinetic analysis by ^1H NMR was difficult because of the complexity and mutual overlap of the aromatic proton signals, ^{13}C dynamic NMR was investigated. At ambient temperature the three benzene rings of the Tp moiety were magnetically equivalent, although the 1/8/13-C and 8a/9a/12-C signals were considerably broadened (Table 1). In compound **5** the interanl motion was frozen at −85 °C and the signals due to the aromatic carbons of the Tp moiety appeared as two sets of peaks with an intensity ratio of 2 : 1 except for the 4/5/16-C signal which remained a single peak because of the very small chemical shift difference between the diastereotopic carbons. None of the signals due to the 2-methylphenyl (Ar) moiety showed splitting nor even

Table 1. ^{13}C Chemical Shifts of Compounds **5** and **6** (δ, 125 MHz, CD_2Cl_2)

Temp/°C	**5**		**6**	
	26	−75	26	−91
Carbon				
2′-CH_3	20.54	20.96	17.51	17.97
CH_2	31.17	30.68	—	—
9	52.57	51.99	86.05	85.23
10	54.74	53.75	53.58	52.46
1	123.90 br	121.29	122.95 br	120.60
8/13		125.15		123.97
2	124.83	125.05	124.94	125.36
7/14		124.50		124.49
3	124.39	125.07	125.85	125.36
6/15		125.43		125.96
4	123.68	123.77	123.60	123.48
5/16				123.89
4a	147.04	147.37	144.28	144.38
10a/11		146.12		143.41
9a	146.1 br	148.70	143.65 br	146.36
8a/12		143.91		141.46
1′	137.81	138.03	154.00	153.36
2′	135.23	135.06	127.50	127.40
3′	130.15	125.95	131.32	131.11
4′	126.08	125.91	121.15	120.82
5′	124.81	124.63	125.43	125.34
6′	131.75	131.35	118.50	117.89

Table 2. ^{13}C Dynamic NMR Data of Compounds **5** and **6** in CD_2Cl_2

	5	**6**
$\Delta H^{\ddagger}$/kcal mol^{-1}	10.7±0.5	9.5±0.3
$\Delta S^{\ddagger}$/cal mol^{-1} K^{-1}	−4.4±2.2	−4.5±1.3
$\Delta G^{\ddagger}_{250K}$/kcal mol^{-1}	11.8	10.7
Temp range/°C	−45——15	−69——45

broadening at the lowest temperature.

A quite similar behavior was observed also for compound **6**, although the spectral change occurred at somewhat lower temperatures than in the case of **5**.

Total lineshape analysis of the 4a/10a/11-C signal was carried out for both compounds in the temperature range shown in Table 2 using the DNMR3 program.[16] Rate constants were determined at five temperatures and the least-squares analysis of the Eyring plot gave the activation parameters which are shown in Table 2.

Interconversion among the stable conformers can take place either by two consecutive GR steps or by a combination of one GR and one IR steps. The former process involves rotation of the Tp–X bond by $4\pi/3$ radian accompanied by rotation of the Ar–X bond by 2π radian by way of an unstable conformer with the *o*-methyl group pointing inward as an intermediate. The latter process involves $2\pi/3$ Tp–X and 2π Ar–X rotations. The relative energy barriers of the GR and IR steps determine the actual process. While the dynamic NMR data do not tell which step has a higher barrier, molecular model considerations strongly favor the GR step.

In order to ascertain this point, we carried out molecular mechanics calculations on these compounds. Table 3 contains the steric energies of the stationary points obtained by the BIGSTRN3 calculation.[17] In either compound, the global minimum conformation is the gear-meshed one with C_S symmetry and the *o*-methyl group pointing outward just as inferred by the molecular model consideration. The conformation with the *o*-methyl group pointing inward is a local minimum with C_1 symmetry, and higher in steric energy by 7—9 kcal mol^{-1} than the global minimum, supporting the absence of the signals ascribable to this conformer in the NMR spectrum. The C_S transition state separates the enantiomeric pair of the C_1 forms with the barrier of 0.01—0.015 kcal mol^{-1}.

The transition state for the GR step is 11.5 and 9.9 kcal mol^{-1} higher than the ground state for **5** and **6**, respectively, and these values well reproduce the experimentally obtained energy barriers. The IR transition state is shown far higher than the GR one in either compound, indicating that the isolated rotation does not contribute to the observed dynamic process.

Table 3. Relative Steric Energies of the Stationary Points of **5** and **6** by BIGSTRN3 Calculations (kcal mol^{-1})[a]

	5		6	
GS/CH_3-out	0.0	C_s	0.0	C_s
GS/CH_3-in	7.08	C_1	9.04	C_1
TS/CH_3-in	7.09	C_s	9.05	C_s
TS/GR	11.50	C_1	9.88	C_1
TS/IR	15.96	C_1	20.12	C_1
HT/IR′	36.49	C_s	68.54	C_s

a) GS: ground state; TS: transition state; HT: hilltop.

Table 3 shows also the energies of the "transition states" of the IR′ process in which the Tp–X bond rotates by $2\pi/3$ without being accompanied by the rotation of the Ar–X bond. These states are of extremely high energy and correspond to the hilltop in the potential energy surface.

Comparison of these molecular mechanics data with those for **3** and **4**[13] reveals that by introduction of an *o*-methyl group the IR barrier increases greatly by 5—6 kcal mol^{-1}, while the GR barrier shows no significant change particularly in **5**.

Syntheses of 7 and 8. Stereoselective Formation of *sc (9*S**) Isomer.** As the target compounds for realization of atropisomerism in 9-(2-methylbenzyl)triptycene derivatives, doubly *peri*-substituted compounds, i.e., 8-chloro-1,4-dimethyl-9-(2-methylbenzyl)triptycene (**7**) and the corresponding 8-bromo compound (**8**) were designed.

Three rotational isomers about the Tp–CH_2 bond are possible for **7** and **8**: *ap*, *sc** (9*S**), and *sc** (9*R**).[18] These are shown in Scheme 1 for the configurational isomer with *S*-configuration at C^9. The *o*-methyl group is considered to point outward by the steric reason. The *sc** (9*R**) (hereafter referred to as *sc2*) form is expected to be less stable than the *ap* and *sc** (9*S**) (hereafter referred to as *sc1*) forms because the 2-methylphenyl group is flanked by two *peri*-substituents.

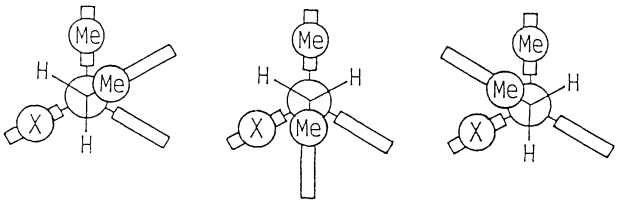

Scheme 1.

Reactions of 1-chloro-9-(2-methylbenzyl) anthracene (**9**) with 3,6-dimethylbenzyne generated in situ by diazotization of 3,6-dimethylanthranilic acid gave 8-chloro-1,4-dimethyl-9-(2-methylbenzyl)triptycene (**7**) in 78% yield. The ^{1}H NMR of the crude product revealed that two rotational isomers **7A** and **7B** were present in a ratio of ca. 9 : 1. Recrystallization of the isomer mixture gave the major isomer **7A** in a pure state. The isomer was stable at ambient temperature with no isomerization even in solution but at higher temperatures isomerization took place to give an equilibrium mixture of the two isomers **7A** and **7B** in a ratio of ca. 1 : 2. Isomer **7A** which was predominant when synthesized was now the minor one. Separation of the two isomers by preparative gel permeation chromatography gave a pure sample of the second isomer **7B**.

Detailed examination of the ^{1}H NMR spectra of the two isomers allowed unambiguous assignments of all the

signals including those of the aromatic protons (Table 4). The structural assignments of the isomers were made as follows. In isomer **7A** the 1-methyl signal appeared at a rather low fieid of δ=2.84. This suggested that the 1-methyl group was located in the plane of the 2-methylphenyl group indicating the *sc1* structure.

Table 4. ^{1}H Chemical Shifts of the Two Isomers of **7** and **8** (500 MHz, $CDCl_3$, 26°C)[a]

	7		**8**	
	sc1 (**A**)	*ap* (**B**)	*sc1* (**A**)	*ap* (**B**)
1-CH_3	2.841s	2.062s	2.851s	2.060s
4-CH_3	2.437s	2.556s	2.437s	2.552s
2'-CH_3	2.590s	2.619s	2.584s	2.643s
CH_2 a	5.324d	4.516d	5.456d	4.481d
	(17.4)	(18.4)	(17.6)	(18.3)
CH_2 b	4.288d	5.267d	4.198d	5.329d
	(17.4)	(18.4)	(17.6)	(18.3)
10-H	5.655s	5.630s	5.639s	5.614s
2-H	6.657d	6.559d	6.663d	6.552d
	(7.9)	(7.9)	(8.1)	(7.7)
3-H	6.668d	6.798d	6.668d	6.794d
	(7.9)	(7.9)	(8.1)	(7.7)
5-H	7.325dd	7.192dd	7.366dd	7.230dd
	(7.1, 1.2)	(7.1, 1.2)	(7.2, 1.2)	(7.2, 1.3)
6-H	6.922dd	6.806dd	6.831t[b]	6.709dd
	(8.0, 7.1)	(8.1, 7.1)	(8.1)	(8.0, 7.2)
7-H	6.853dd	6.962dd	7.093dd	7.194dd
	(8.0, 1.3)	(8.1, 1.3)	(7.9, 1.3)	(8.0, 1.2)
13-H	7.063brd	7.050brd	7.079d	7.035d
	(7.7)	(7.8)	(7.6)	(7.7)
14-H	6.828td	6.829td	6.829t[b]	6.824td
	(7.7, 1.2)	(7.6, 1.3)	(8.1)	(7.7, 1.3)
15-H	7.026td	7.035td	7.032td	7.034td
	(7.4, 0.9)	(7.4, 0.9)	(7.4, 1.0)	(7.4, 1.0)
16-H	7.429dd	7.438dd	7.431dd	7.436dd
	(7.4, 1.2)	(7.2, 1.0)	(7.3, 1.1)	(7.5, 1.3)
3'-H	7.271brd	7.282brd	7.275brd	7.282brd
	(7.4)	(7.4)	(7.4)	(7.4)
4'-H	7.080brt	7.073brt	7.092brt	7.068brt
	(7.3)	(7.4)	(7.6)	(7.4)
5'-H	6.738brt	6.702brt	6.737brt	6.688brt
	(7.6)	(7.6)	(7.6)	(7.4)
6'-H	6.498brd	6.459brd	6.451brd	6.420brd
	(7.8)	(7.9)	(7.8)	(7.9)

a) Chemical shifts are given in δ. In parentheses are coupling constants in Hz. b) Mutually interchangeable.

Irradiation of the 1-methyl protons caused the increase in the signal intensity of both of the methylene protons (the nuclear Overhauser effect), indicating the proximity of both protons to the 1-methyl group in agreement with the above assignment. On the other hand the 1-methyl group of **7B** resonated at a high field of δ=2.06 suggesting that the 1-methyl group was located above the plane of the 2-methylphenyl group. Irradiation of the 1-methyl protons increased the signal intensity of the lower-field proton (H^b) of the methylene group. These facts clearly suggested that **7B** was the *ap* isomer.

The third possible rotamer, *sc** (9*R**), was not detected at all in agreement with the supposition by molecular models.

Similar reaction of 1-bromo-9-(2-methylbenzyl)anthracene (**10**) with 3,6-dimethylbenzyne gave 8-bromo-1,4-dimethyl-9-(2-methylbenzyl)triptycene (**8**) in 90% yield, which was shown to be composed of two rotational isomers **8A** and **8B** in a ratio of >95:<5. Recrystallization of the isomer mixture gave a pure sample of the major isomer **8A**. Thermal equilibration followed by chromatographic separation of the isomer mixture (**8A** : **8B**=3 : 7) allowed the isolation of the other isomer **8B**. Detailed analysis of the ^{1}H NMR spectra of the isomers assigned *sc1* and *ap* to **8A** and **8B**, respectively, on the basis of the similar reasoning as in the case of compound **7**.

Stereoselective formation of the *sc1* isomer in either of **7** and **8** upon synthesis is consistent with the general rule hitherto observed in the formation of atropisomers by reactions of 9-substituted anthracenes with dienophiles such as benzyne derivatives: The bulkiest side-chain in the 9-substituent assumes the farthest position from the entering dienophile moiety.[3,4,7,8]

Rotamer Isomerization in 7 and 8. Kinetic studies of the *sc1* $\rightleftharpoons$ *ap* isomerization of **7** and **8** in toluene-d_8 was carried out starting from the pure *sc1* isomer in the temperature range of 50—90°C. The kinetic parameters obtained therefrom are given in Table 5.

For the 8-bromo compound **8** the rate constant is about three times smaller and the energy barrier is about 0.9 kcal mol^{-1} higher than those for the chloro compound **7**. This may be reasonable if we admit that the bulkier

Table 5. Kinetic Data for Isomerization of **7** and **8** in Toluene-d_8[a]

7				**8**			
Temp	K	k	$\Delta G^{\ddagger}$	Temp	K	k	$\Delta G^{\ddagger}$
°C	[*ap*]/[*sc1*]	10^{-5} s^{-1}	kcal mol^{-1}	°C	[*ap*]/[*sc1*]	10^{-5} s^{-1}	kcal mol^{-1}
50.0	1.87	1.08	26.31	54.0	2.27	0.501	27.15
60.0	1.86	3.74	26.33	66.0	2.26	2.16	27.18
70.0	1.85	11.5	26.37	78.0	2.25	8.68	27.20
80.0	1.82	35.5	26.37	90.0	2.24	30.2	27.25
90.0	1.81	94.1	26.43				
$\Delta H^{\ddagger}$=25.4±0.6 kcal mol^{-1}				$\Delta H^{\ddagger}$=26.3±0.6 kcal mol^{-1}			
$\Delta S^{\ddagger}$=−2.7±1.8 cal mol^{-1} K^{-1}				$\Delta S^{\ddagger}$=−2.7±1.8 cal mol^{-1} K^{-1}			

a) Values for the *sc1* to *ap* process.

bromo substituent destabilizes the transition state for isomerization more than the ground state whatever the transition state is. The isomerization mechanism will be considered in detail in the next section.

The composition of rotamers at equilibrium is also worth consideration. The 8-bromo compound **8** has a larger equilibrium constant ([*ap*]/[*sc1*]) than the 8-chloro compound **7**, suggesting that the repulsive van der Waals interaction between the halogen and the 2-methylphenyl group is important in determining the equilibrium position (see the Newman projections in Scheme 1). As it is usually recognized that methyl is bulkier than chloro and bromo (van der Waals radii are 2.0, 1.75, and 1.85 Å, respectively, according to Pauling[19]), the equilibrium constants smaller than unity will be expected for both compounds if only the steric factor is considered. The observed values of greater than unity suggest the operation of some additional factors, e.g., electrostatic repulsion between the halogen and the π-electrons of the 2-methylphenyl group and/or attractive interaction between the 1-methyl group and the 2-methylphenyl group, such as C–H···π interaction.[20]

Isomerization Pathways. Interconversion between the two isomers, *ap* and *sc1*, of compounds **7** and **8** can occur by several pathways, each of which is a combination of GR and/or IR steps as shown in Scheme 2. Two pathways which consist only of GR steps are available: (a) *ap*⇌*sc2'*⇌*sc1* and (b) *ap*⇌*sc1'*⇌*sc2*⇌*ap'*⇌*sc1*. The former pathway requires the rotation of the Tp–CH_2 bond by $4\pi/3$ and the Ar–CH_2 bond of 2π while the latter requires $8\pi/3$ rotation of the Tp–CH_2 bond and 4π rotation of the Ar–CH_2 bond. Four pathways involving an IR step are possible: (c) *ap*⇌*sc1'*⇌*sc1*, (d) *ap*⇌*ap'*⇌*sc1*, (e) *ap*⇌*sc1'*⇌*sc2*⇌*sc2'*⇌*sc1*, and (f) *ap*⇌*sc2'*⇌*sc2*⇌*ap'*⇌*sc1*.

It is difficult to infer which of these pathways has the lowest energy barrier and actually takes place, although pathways (e) and (f) may be easily excluded by simple molecular model considerations because IR in the *sc2* isomer seems highly unlikely to occur.

The experimental results do not give the answer, nor is the *peri*-substituent effect on the barrier heights is useful to distinguish the pathways.

Molecular Mechanics Calculations on 7. In order to obtain information on the pathways of the rotamer interconversion, molecular mechanics calculation was carried out on compound **7** using the BIGSTRN3 program.[17] The steric energies of the stationary points are compiled in Table 6.

As for the energy minima, the calculated results are completely consistent with the experimental ones. The *ap* rotamer corresponds to the global energy minimum and the *sc1* rotamer is slightly less stable than *ap*, while *sc2* is far less stable. The conformers with the *o*-methyl

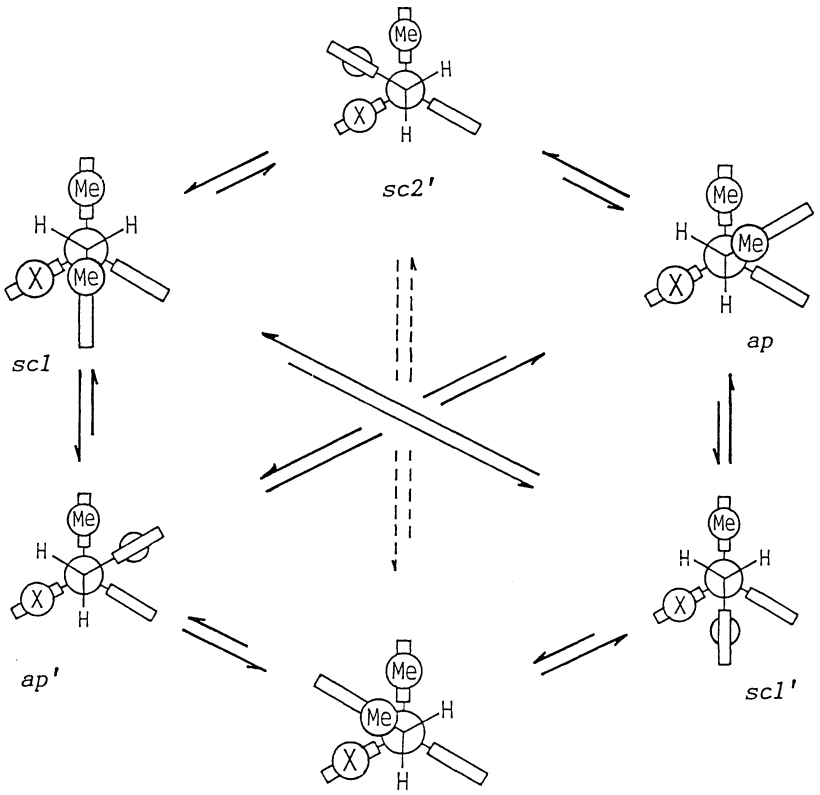

Scheme 2.

Table 6. Relative Steric Energies of Stationary Points in **7** by BIGSTRN3[a)]

GS		TS (GR)		TS (IR)	
ap	0.0	*ap* ⇌ *sc1'*	18.366	*ap* ⇌ *ap'*	33.484[b)]
sc1	0.187	*sc1* ⇌ *ap'*	18.686		34.465[c)]
sc2	3.873	*ap* ⇌ *sc2'*	27.724	*sc1* ⇌ *sc1'*	31.003[b)]
ap'	6.779	*sc2* ⇌ *ap'*	24.093		31.354[d)]
sc1'	7.150	*sc1* ⇌ *sc2'*	29.131	*sc2* ⇌ *sc2'*	46.047[c)]
sc2'	10.143	*sc2* ⇌ *sc1'*	25.835		46.068[d)]

a) Energies are given in kcal mol^{-1} relative to *ap*. GS: ground state. TS: transition state. b) The 2'-methyl group is close to the 13-hydrogen. c) The 2'-methyl group is close to the 1-methyl group. d) The 2'-methyl group is close to the 8-chloro group.

group pointing inward, designated as *ap'*, *sc1'*, and *sc2'*, respectively, are 6—7 kcal mol^{-1} less stable than the corresponding methyl-outward conformers.

The transition states for the *ap*⇌*sc1'* and *sc1*⇌*ap'* GR processes in which the Ar group passes over the *peri*-hydrogen lie about 18.5 kcal mol^{-1} above the global minimum.

The transition states for the GR processes in which the Ar group passes over the *peri*-methyl group (*ap*⇌*sc2'* and *sc2*⇌*ap'*) or over the *peri*-chloro group (*sc1*⇌*sc2'* and *sc2*⇌*sc1'*) are much higher in energy. It is interesting that the GR barriers are significantly dependent on which is the more stable *o*-methyl-outward form, e.g. the barrier to the *ap*⇌*sc2'* process is 3.6 kcal mol^{-1} higher than that to the *sc2*⇌*ap'* process.

The energy barriers to the pathways (a) and (b) are thus calculated as 29.13 and 25.84 kcal mol^{-1}, respectively. The passing of Ar over the *peri*-chloro group is the rate-determining step in either pathway. This may be compatible with the inference that the repulsive interaction between the *peri*-substituent and the face of the Ar group at the transition state is larger with the *peri*-Cl than with the *peri*-CH_3 as discussed in the previous section.

The IR process has two routes in each site depending on the clockwise and counterclockwise rotation of the Ar group. The energy barrier difference between the two routes is small and at most 1 kcal mol^{-1}. The energy barriers to the pathways (c) and (d) are calculated as 31.00 and 33.48 kcal mol^{-1}, respectively, with the IR step being the rate-determining step. The barriers for (e) and (f) are 46.05 kcal mol^{-1} and far higher than those for the other pathways.

Therefore the present molecular mechanics calculation suggests that the interconversion between the *ap* and *sc1* rotamers of **7** takes place by the pathway (b). The calculated energy barrier to the *sc1*→*ap* conversion is 25.65 kcal mol^{-1} and agrees excellently with the experimentally obtained enthalpy of activation, 25.4 kcal mol^{-1} (Table 5). It is interesting to note that the pathway (b) is highly roundabout with four GR steps but has the lowest energy barrier.

Solid State Behavior of 7 and 8.[15b)] Differential scanning calorimetric (DSC) studies were carried out for rotameric crystals of **7** and **8**, and some of the DSC diagrams are shown in Figs. 1 and 2.

The *ap* isomer of **7** showed a strong endothermic peak (ca. 8.5 kcal mol^{-1}) at 242°C, which corresponded to the melting point (mp) of *ap*-**7** obtained by the conventional mp measurement, irrespective of the scan rate (Fig. 1a). On the contrary, the thermal behavior of *sc1*-**7** depended on the scan rate. When scanned rapidly (180°C h^{-1}), an endothermic peak (ca. 7.6 kcal mol^{-1}) was observed at 216°C, mp of *sc1*-**7** (Fig. 1b). When scanned slowly (20°C h^{-1}), only a weak broad exothermic peak (ca. 0.5 kcal mol^{-1}) was observed at 214°C and instead a

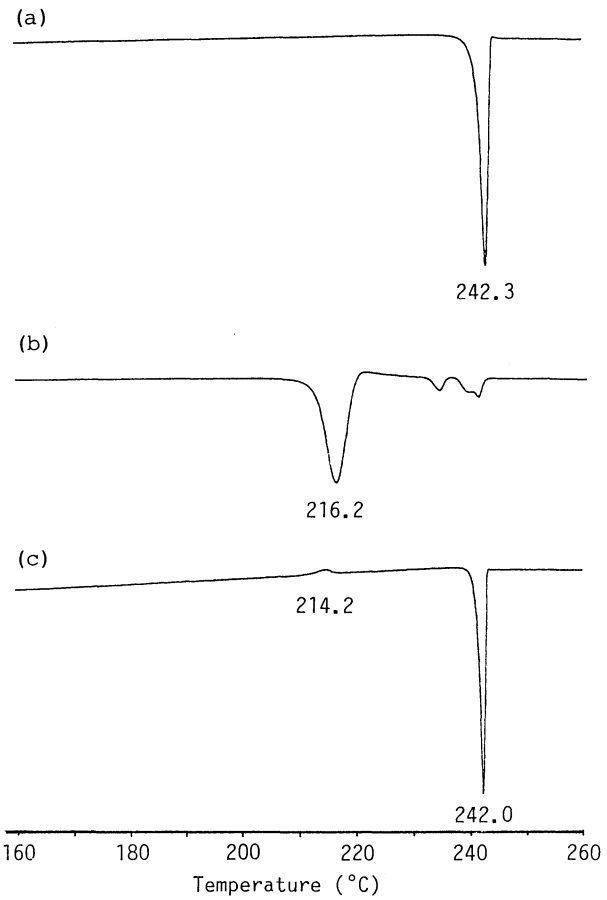

Fig. 1. DSC diagrams of **7**. (a) *ap*-**7**, 60°C h^{-1}; (b) *sc1*-**7**, 180°C h^{-1}; (c) *sc1*-**7**, 20°C h^{-1}.

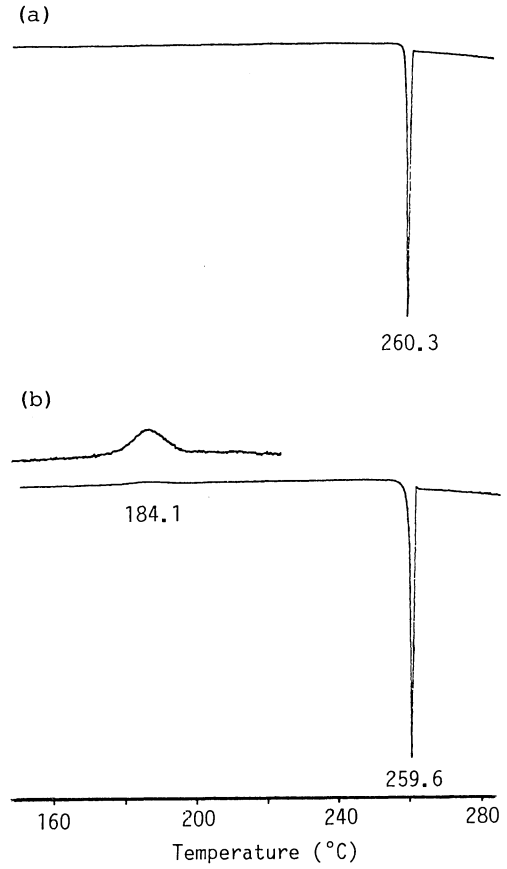

Fig. 2. DSC diagrams of **8**. (a) *ap*-**8**, 60°C h^{-1}; (b) *scl*-**8**, 60°C h^{-1}.

strong endothermic peak (ca. 9.4 kcal mol^{-1}) appeared at 242°C (Fig. 1c). At an intermediate scan rate (60°C h^{-1}), the diagram looked like a superposition of these two extreme diagrams.

The data suggested that the crystalline *ap*-**7** retained its identity until it melted at 242°C, while the crystalline *scl*-**7** melted at 216°C when heated rapidly but when heated slowly it entirely isomerized to *ap*-**7** at about 215°C without melting and then melted at 242°C, when the actual species was *ap*-**7**.

To confirm this hypothesis, 1—2 mg portions of pure atropisomeric crystals were placed in capillary tubes and were heated in a metal heating block for the mp measurement under various conditions. The isomer composition of the samples was then determined by ^{1}H NMR in $CDCl_3$.

The *ap*-**7** crystals showed no isomerization at all below 242°C, mp of this isomer. When heated above this temperature, the crystals melted and gave a glass when cooled to room temperature, the ^{1}H NMR spectrum of which showed that it consisted of *scl* and *ap* rotamers in a ratio of ca. 3 : 2, presumably reflecting the equilibrium composition in the melt.

The *scl* isomer showed a complex behavior. When a sample of *scl*-**7** was inserted into the heating block that had been preheated at 220°C, the crystals immediately melted to a clear liquid but in a few seconds it solidified. After heated at this temperature for 1 h, the sample was withdrawn, cooled, and subjected to ^{1}H NMR measurement in $CDCl_3$ at 26°C, which showed that the sample was an isomer mixture with the *ap*/*scl* ratio of 7.6 (*scl*-**7**: 12%). When a sample of *scl*-**7** was inserted to the block preheated at 185°C and the temperature was slowly raised to 220°C at 6°C h^{-1}, no change in the appearance of the solid was observed but a mixture with the rotamer ratio of 8.0 was obtained.

When a sample of *scl*-**7** was inserted into the block at 200°C, a temperature below the mp of *scl*-**7**, and kept at this temperature, slow isomerization took place without any change of the appearance. The isomer ratio was 0.14 after 5 min and 0.36 after 15 min, and finally reached 13.1 (*scl*-**7**: 7%) after 4 h. Although the mechanistic details of the isomerization are yet unknown, if a first-order irreversible reaction is assumed, the change at the early stage gives $k=(4.0\pm0.5)\times10^{-4}$ s^{-1} which corresponds to $\Delta G^{\ddagger}$ of ca. 35.5 kcal mol^{-1}.

The DSC diagram of *ap*-**8** showed an intense endothermic peak (ca. 8.9 kcal mol^{-1}) at 260.3°C irrespective of the scan rate (Fig. 2a), while *scl*-**8** gave an endothermic peak (ca. 8.3 kcal mol^{-1}) at 260°C and in addition a small broad exothermic peak (ca. 0.5 kcal mol^{-1}) at 180—190°C region irrespective of the scan rate (20 to 180°C h^{-1}) (Fig. 2b). These data suggested that the crystalline *ap*-**8** melted at 260°C, while the *scl* isomer entirely isomerized to *ap* at ca. 185°C without melting and then melted at 260°C, when the solid existed as the *ap* isomer.

This was again confirmed by the isomerization experiments in which the atropisomeric crystals of **8** were heated under various conditions.

The *ap*-**8** samples did not isomerize at all below 260°C, its mp. When a sample of *scl*-**8** was inserted into the heating block preheated at 160°C and was heated at a rate of ca. 30°C h^{-1} to 250°C, no change of the appearance of the solid was detected. The ^{1}H NMR spectrum of the sample showed the *ap*/*scl* ratio of 13.3 (*scl*-**8**: 7%). When an *scl*-**8** sample was inserted into the heating block preheated at 250°C, it immediately melted to a clear liquid but in a few seconds it solidified to a waxy solid. Additional heating of the sample at 250°C for 15 min showed no further change of the appearance. The ^{1}H NMR spectrum showed the *ap*/*scl* ratio of 6.30 (*scl*-**8**: 14%).

These findings as well as the DSC data indicated the mp of 259—260°C observed for *scl*-**8** was really that of *ap*-**8** and the "intrinsic" mp of *scl*-**8** might be around 185°C and that rapid heating of *scl*-**8** above this temperature resulted in melting but slow heating caused isomerization to *ap*-**8** without melting.

When *scl*-**8** crystals were placed in the block at 170°C, slow isomerization took place. The *ap*/*scl* ratio was 0.18 and 0.70 after 40 and 150 min, respectively. The first-order rate constant at the early stage was calculated to be $(6.5\pm0.5)\times10^{-5}$ s^{-1} which corresponded to $\Delta G^{\ddagger}$ of

Table 7. Crystal Data of Rotamers of **7** and **8**

	ap-**7**	*scl*-**7**	*ap*-**8**	*scl*-**8**
Crystal form	Triclinic	Monoclinic	Triclinic	Tetragonal
Space group	$P\bar{1}$	$P2_1/a$	$P\bar{1}$	$I4_1/a$
a/Å	10.028(1)	23.803(3)	10.070(1)	27.746(1)
b/Å	15.773(1)	8.465(1)	15.925(1)	27.746
c/Å	15.601(2)	11.083(2)	15.582(2)	11.817(3)
α/deg	114.715(8)	90.0	115.032(9)	90.0
β/deg	102.02(1)	98.13(4)	102.59(2)	90.0
γ/deg	78.189(9)	90.0	78.09(1)	90.0
V/Å^3	2170.9(9)	2211(1)	2191.2(9)	9097(2)
Z	4	4	4	16
R	0.078	0.093	0.057	0.072

ca. 35 kcal mol^{-1}.

As for the practical aspect, the present finding affords a simple way to isolate the *ap*-isomer of **7** or **8**. Instead of tedious chromatographic separation of the isomers from the equilibrated isomer mixture, heating a crystalline sample, either the pure *scl* isomer or a mixture of isomers, at an appropriate temperature gives an *ap*-rich mixture, recrystallization of which gives a pure sample of the *ap* isomer.

X-Ray Crystallographic Studies. The ease of the irreversible isomerization in solid state may be related to the crystal structures and packings of the isomeric crystals. X-Ray crystallographic studies were thus carried out on the rotameric crystals of both **7** and **8**. Details of the analysis were separately reported.[21] The crystal data are given in Table 7.

The crystal structures of the two *ap*-isomers, *ap*-**7** and *ap*-**8**, are isomorphous to each other, both in the triclinic form. The *scl*-**7** crystal is monoclinic, and two enantiomeric molecules occupy one site in a 3 : 1 ratio resulting in a disordered form. *scl*-**8** exists in a tetragonal form and one site is occupied by one of the enantiomers and no disorder is observed. Anyway, the crystal structures are completely different between *ap* and *scl* isomers for both **7** and **8**. These facts suggest that the crystal would be destroyed during thermal isomerization from *scl* to *ap* in the crystalline state, although no change in the appearance was visually detected. The irreversibility of the isomerization may be a reflection of the fact that molecules are more densely packed in the *ap* crystal than in the *scl* crystal for both compounds.

The molecular structures of the two isomers of **7** are close to those obtained by the molecular mechanics calculations mentioned above, and no unusual bond lengths and angles are found. The structures of the isomers of **8** are very similar to the respective counterparts of **7**.

Table 8. ^{13}C Chemical Shift Data of **7** and **8** (δ, 125 MHz, $CDCl_3$, 26°C)[a]

	7		**8**	
	scl	*ap*	*scl*	*ap*
1-CH_3	23.82	21.42	23.81	21.43
4-CH_3	18.98	18.84	18.96	18.81
2′-CH_3	20.86	20.79	20.95	21.14
CH_2	35.62	35.84	35.34	36.33
9	56.97	56.78	57.36	56.64
10	51.81	52.02	51.98	52.19
2	130.29	129.75	130.32	129.75
3	126.54	127.14	126.54	127.14
5	122.30	122.61	122.93	123.23
6	126.48	125.82	126.64	126.07
7	129.83	129.22	132.53	132.88
8	131.04	128.90	119.61	116.47
13	127.01	127.18	127.24	127.22
14	124.29	124.23	124.30	124.23
15	125.57	125.63	125.64	125.66
16	122.79	122.84	122.75	122.82
3′	129.47	129.60	129.51	129.59
4′	125.28	125.56	125.33	125.55
5′	124.80	124.88	124.80	124.84
6′	128.78	128.85	129.24	128.85
quat.	129.83	129.13	129.83	129.11
	130.43	132.77	130.47	132.79
	135.87	136.31	136.02	136.40
	138.72	138.29	138.56	138.11
	141.52	142.00	143.16	141.88
	144.70	143.76	144.55	143.96
	144.73	144.02	144.68	144.72
	145.10	144.78	145.04	144.85
	146.70	145.01	146.63	145.32
	148.88	151.75	149.20	152.04

a) Most of the quaternary carbons are not assigned.

Experimental

Melting points were measured on a MELTEMP apparatus and are not corrected. ^{1}H NMR spectra were obtained on a Varian EM-390 spectrometer operating at 90.0 MHz in the CW mode or on a Bruker AM-500 spectrometer operating at 500.1 MHz in the pulse FT mode with internal tetramethylsilane (TMS) as the chemical shift standard. For triptycenes, the signals were unambiguously assigned on the basis of homonuclear decoupling and nuclear Overhauser effect (NOE) experiments unless otherwise stated. ^{13}C NMR spectra were

recorded on AM-500 at 125.8 MHz. Most of the signals derived from protonated carbons were unambiguously assigned by ^{13}C–^{1}H COSY experiments. Preparative gel permeation chromatography (GPC) was performed on an LC-09 Liquid Chromatograph (Japan Analytical Industry Co., Ltd.) using a series of JAIGEL 1H and 2H columns and chloroform as the eluent. Differential scanning calorimetry was performed on a Rigaku Thermal Analysis Station TAS-100 equipped with a DSC-8230 calorimeter using alumina as the reference sample.

9-(2-Methylbenzyl) triptycene (5). To a solution of 282 mg (1.0 mmol) of 9-(2-methylbenzyl)anthracene[14b] in 10 ml of 1,2-dimethoxyethane (DME) were added simultaneously a solution of 550 mg (4.0 mmol) of anthranilic acid in 30 ml of DME and a solution of 1 ml (ca. 7.5 mmol) of isopentyl nitrite in 30 ml of DME during the course of 1.5 h and the mixture was heated under reflux for further 0.5 h. After evaporation of the solvent, the residue was chromatographed through alumina with hexane as the eluent and then recrystallized from dichloromethane–hexane to give 279 mg (77%) of **5**, mp 282—283 °C. Found: C, 93.66; H, 6.49%. Calcd for $C_{28}H_{22}$: C, 93.81; H, 6.19%. ^{1}H NMR ($CDCl_3$, 500 MHz) δ=2.684 (3H, s, CH_3), 4.233 (2H, s, CH_2), 5.453 (1H, s, 10-H), 6.82—6.93 (5H, m, 5′-H, 6′-H, and 2/7/14-H), 6.982 (3H, t, J=7.4 Hz, 3/6/15-H), 7.134 (1H, dt, J=1.6 and 7.0 Hz, 4′-H), 7.209 (3H, br d, J=6.9 Hz, 1/8/13-H), 7.322 (1H, d, J=7.6 Hz, 3′-H), 7.412 (3H, d, J=7.3 Hz, 4/5/16-H). ^{13}C NMR ($CDCl_3$) δ=20.43 (CH_3), 30.95 (CH_2), 52.15 (9-C), 54.52 (10-C), 123.32 (4/5/16-C), ca. 123.6 (br, 1/8/13-C), 124.49 (2/7/14-C), 124.70 (5′-C), 124.96 (3/6/15-C), 125.72 (4′-C), 129.73 (3′-C), 131.64 (6′-C), 134.84 (2′-C), 137.14 (1′-C), ca. 145.6 (br, 8a/9a/12-C), 146.61 (4a/10a/11-C).

9-(2-Methylphenoxy)triptycene (6). To a solution of 1.14 g (4.0 mmol) of 9-(2-methylphenoxy)anthracene[22] in 20 ml of acetone were simultaneously added a solution of 2.74 g (20 mmol) of anthranilic acid in 50 ml of acetone and a solution of 4 ml (ca. 30 mmol) of isopentyl nitrite in 50 ml of acetone during the course of 3 h and the mixture was heated under reflux for further 0.5 h. After evaporation of the solvent, the residue was chromatographed through alumina with dichloromethane–hexane (1 : 8) as the eluent to give 749 mg (52%) of **6** after recrystallization from dichloromethane–hexane, mp 211—212 °C. Found: C, 90.03; H, 5.74%. Calcd for $C_{27}H_{20}O$: C, 89.97; H, 5.59%, ^{1}H NMR ($CDCl_3$, 500 MHz) δ=2.730 (3H, s, CH_3), 5.410 (1H, s, 10-H), 6.636 (1H, d, J=8.0 Hz, 6′-H), 6.882 (1H, dt, J=1.8 and 7.7 Hz, 5′-H), 6.929 (1H, dt, J=1.0 and 7.4 Hz, 4′-H), 6.949 (3H, dt, J=1.3 and 7.4 Hz, 2/7/14-H), 7.002 (3H, dt, J=1.3 and 7.4 Hz, 3/6/15-H), 7.340 (1H, dd, J=1.0 and 7.3 Hz, 3′-H), 7.403 (3H, dd, J=0.8 and 7.3 Hz, 4/5/16-H), 7.414 (3H, brd, J=7.4 Hz, 1/8/13-H). ^{13}C NMR ($CDCl_3$) δ=17.40 (CH_3), 53.38 (10-C), 85.74 (9-C), 118.28 (6′-C), 120.70 (4′-C), 122.72 (br, 1/8/13-C), 123.17 (4/5/11-C), 124.59 (2/7/14-C), 125.20 (5′-C), 125.40 (3/6/15-C), 127.03 (2′-C), 130.90 (3′-C), 143.55 (br, 8a/9a/12-C), 143.85 (4a/10a/11-C), 153.67 (1′-C).

sc (9S*)-8-Chloro-1,4-dimethyl-9-(2-methylbenzyl)triptycene (**sc1**-7).* To a solution of 634 mg (2.0 mmol) of 1-chloro-9-(2-methylbenzyl)anthracene (**9**)[14b] in 30 ml of acetone were added simultaneously a solution of 420 mg (2.5 mmol) of 3,6-dimethylanthranilic acid[23] in 50 ml of acetone and a solution of 0.6 ml (ca. 4.5 mmol) of isopentyl nitrite in 50 ml of acetone during the period of 1 h and the mixture was heated under reflux for 15 min. After evaporation of the solvent, the residue was chromatographed on an alumina column with hexane–dichloromethane as the eluent to give a mixture of the *sc** (9*S**) and *ap* isomers in a ratio of ca. 9 : 1 with a total yield of 78%. Recrystallization of the mixture from dichloromethane–hexane gave a pure sample of *sc** (9*S**)-**7**, mp 217—219 °C. Found: C, 85.69; H, 6.11; Cl, 8.40%. Calcd for $C_{30}H_{25}Cl$: C, 85.59; H, 5.99; Cl, 8.42%. See Tables 4 and 8 for the ^{1}H and ^{13}C NMR data, respectively.

***ap*-8-Chloro-1,4-dimethyl-9-(2-methylbenzyl)triptycene (*ap*-7).** (A) A solution of *sc1*-**7** in toluene was heated at 80 °C for 20 h to give a mixture of *sc1*-**7** and *ac*-**7** in a ratio of ca. 1 : 2. The mixture was subjected to preparative GPC. Fifty recycles gave two slightly overlapping peaks, the major component (*ap*-**7**) moving slower. Recrystallization of the later fractions of the eluate from dichloromethane–hexane gave a pure sample of *ap*-**7**, mp 240—241 °C. See Tables 4 and 8 for the ^{1}H and ^{13}C NMR data, respectively.

(B) A 128 mg (0.30 mmol) portion of crystalline *sc1*-**7** was heated in a small test tube at 200 °C for 3 h using an oil bath to give a mixture of *ap*-**7** and *sc1*-**7** in a ratio of 93 : 7. Recrystallization of the solid from dichloromethane–hexane gave 107 mg of pure (>98%) *ap*-**7**.

1-Bromo-9-(2-methylbenzyl)anthracene (10). To a Grignard reagent prepared from 0.62 g (4.4 mmol) of 2-methylbenzyl chloride and 122 mg (5 mmol) of magnesium in 30 ml of diethyl ether was added all at once 1.09 g (4.0 mmol) of 1-bromoanthrone[24] as powdery solids, and the mixture was stirred at room temperature for 30 min and then heated under reflux for 30 min. After cooled to room temperature, the mixture was treated with saturated aqueous ammonium chloride to form inorganic solids and a clear organic solution. The solution was separated by decantation and the solids were washed with diethyl ether. The combined ethereal solution was concentrated to give crude 1-bromo-9,10-dihydro-9-(2-methylbenzyl)-9-anthrol as yellow oil: ^{1}H NMR ($CDCl_3$, 90 MHz) δ=1.50 (3H, s), 2.72 (1H, d, J=19.2 Hz), 3.25 (1H, d, J=12.8 Hz), 3.54 (1H, d, J=19.2 Hz), 3.65 (1H, d, J=12.8 Hz), 3.81 (1H, s, OH), 6.26 (1H, br d, J=6.9 Hz), 6.5—7.4 (8H, m), 7.51 (1H, m), 7.80 (1H, m).

Without further purification, the oil was dissolved in 30 ml of benzene containing 1 ml of pyridine. To the solution was added 0.3 ml (4.1 mmol) of thionyl chloride and the mixture was heated on a water bath for 5 min. The mixture was treated with water and the organic layer was washed successively with dilute hydrochloric acid, water, and saturated aqueous sodium chloride, dried over magnesium sulfate, and concentrated. The residue was subjected to column chromatography on alumina with hexane as the eluent to give 1.07 g (74%) of **10** as pale yellow crystals, mp 135—137 °C (from tetrahydrofuran–hexane). Found: C, 73.06; H, 4.72; Br, 22.51%. Calcd for $C_{22}H_{17}Br$: C, 73.14; H, 4.74; Br, 22.12%. ^{1}H NMR ($CDCl_3$, 90 MHz) δ=2.49 (3H, s), 5.12 (2H, s), 6.4—8.1 (11H, m), 8.35 (1H, s).

sc (9S*)-8-Bromo-1,4-dimethyl-9-(2-methylbenzyl)triptycene (**sc1**-8).* The same procedure as in the synthesis of *sc1*-**7** was followed starting from 722 mg (2.0 mmol) of 1-bromo-9-(2-methylbenzyl)anthracene. Column chromatography of the product through alumina with hexane–dichloromethane as the eluent gave a mixture of the *sc** (9*S**)-**8** and *ap*-**8** with a ratio of >95 : <5 in the total yield of 90%. Recrystallization of the mixture from dichloromethane–hexane gave a pure sample of *sc** (9*S**)-**8**, mp 259—260 °C. Found: C, 77.16; H, 5.44; Br,

17.62%. Calcd for $C_{30}H_{25}Br$: C, 77.42; H, 5.41; Br, 17.17%. See Tables 4 and 8 for the ^1H and ^{13}C NMR data, respectively.

***ap*-8-Bromo-1,4-dimethyl-9-(2-methylbenzyl)triptycene (*ap*-8).** (A) A solution of *sc1*-**8** in toluene was heated at 80 °C for 20 h to give a mixture of *sc1*-**8** and *ap*-**8** in a ratio of ca. 3 : 7. The mixture was subjected to preparative GPC. Fifty recycles gave two baseline-separated peaks, the major component (*ap*-**8**) being eluted later. Recrystallization of the later eluate from dichloromethane–hexane gave a pure sample of *ap*-**8**, mp 260—261 °C. See Tables 4 and 8 for the ^1H and ^{13}C NMR data, respectively.

(B) A 93 mg (2.0 mmol) portion of crystalline *sc1*-**8** was heated at 200 °C for 3 h and cooled to give a mixture of *ap*-**8** and *sc1*-**8** in a ratio of 9 : 1. Recrystallization of the solids from dichloromethane–hexane gave 70 mg of pure (>98%) *ap*-**8**.

Total Lineshape Analysis. Total lineshape analysis of the variable-temperature ^{13}C NMR spectra of compounds **5** and **6** was carried out on an NEC PC-9801VX personal computer equipped with a Graphtec MIPLOT II plotter using the DNMR3K program, a modified version of DNMR3[16] converted for use on personal computers by Prof. H. Kihara of Hyogo University of Teacher Education. The signals due to the 4a/10a/11-carbons were analyzed as a one-spin three-site system with mutual exchange. Temperature dependence of the chemical shift difference was properly taken into account.

Classical Kinetic Studies. An NMR sample tube containing a solution of the *sc1* rotamer of **7** or **8** in toluene-d_8 (ca. 10 mg/0.5 ml) was immersed in a thermostated water bath and was withdrawn at appropriate intervals to obtain ^1H NMR spectra at 26 °C. The change in the relative intensities of the methyl signals were followed and the data were analyzed assuming a reversible first-order process[4] to give the rate constant for the *sc1*→*ap* isomerization shown in Table 5.

Molecular Mechanics Calculations. Molecular mechanics calculations were performed using the BIGSTRN3 program[17] on a Hitac M-682H computer system at the Computer Center of the University of Tokyo. Several force field parameters were modified or added as described before.[13] Whether the obtained saddle-point structures actually corresponded to the transition state of interconversion between two energy minima was confirmed by performing the eigenvector distortion option of the program.

In the preliminary calculations on **7**, a higher-energy structure was erroneously assigned to the *sc1*⇌*sc2'* transition state and thus it was concluded that the pathway (a) was the lowest energy path.[15a] The more detailed and careful studies revealed that the earlier conclusion was wrong.

The authors are grateful to Mr. Katsuya Inoue, The University of Tokyo, for the DSC measurements. The present work was supported by a Grant-in-Aid for Scientific Research on Priority Areas No. 03214107 from the Ministry of Education, Science and Culture.

References

1) E. L. Eliel, "Stereochemistry of Carbon Compounds," McGraw-Hill, New York (1962), pp. 156—178.
2) M. Ōki, *Top. Stereochem.*, **14**, 1 (1983).
3) M. Ōki and G. Yamamoto, *Chem. Lett.*, **1972**, 45.
4) G. Yamamoto and M. Ōki, *Bull. Chem. Soc. Jpn.*, **48**, 2592 (1975).
5) H. Iwamura, *J. Chem. Soc., Chem. Commun.*, **1973**, 232.
6) G. Yamamoto and M. Ōki, *Bull. Chem. Soc. Jpn.*, **48**, 3686 (1975).
7) S. Otsuka, T. Mitsuhashi, and M. Ōki, *Bull. Chem. Soc. Jpn.*, **52**, 3663 (1979); S. Otsuka, G. Yamamoto, T. Mitsuhashi, and M. Ōki, *Bull. Chem. Soc. Jpn.*, **53**, 2095 (1980).
8) G. Yamamoto, M. Suzuki, and M. Ōki, *Angew. Chem., Int. Ed. Engl.*, **20**, 607 (1981); *Chem. Lett.*, **1980**, 1523; *Bull. Chem. Soc. Jpn.*, **56**, 306, 809 (1983).
9) K. Yonemoto, F. Kakizaki, G. Yamamoto, and M. Ōki, *Bull. Chem. Soc. Jpn.*, **58**, 3346 (1985); T. Tanaka, K. Yonemoto, Y. Nakai, G. Yamamoto, and M. Ōki, *ibid.*, **61**, 3239 (1988); M. Ōki, T. Tanuma, and G. Yamamoto, *ibid.*, **61**, 4309 (1988).
10) L. H. Schwartz, C. Koukotas, and C. S. Yu, *J. Am. Chem. Soc.*, **99**, 7710 (1977); L. H. Schwartz, C. Koukotas, P. Kukkola, and C. S. Yu, *J. Org. Chem.*, **51**, 995 (1986).
11) C. Rüchardt and H.-D. Beckhaus, *Angew. Chem., Int. Ed. Engl.*, **24**, 529 (1985); M. A. Flamm-ter Meer, H.-D. Beckhaus, K. Peters, H.-G. von Schnering, H. Fritz, and C. Rüchardt, *Chem. Ber.*, **119**, 1492 (1986).
12) a) G. Yamamoto and M. Ōki, *Angew. Chem., Int. Ed. Engl.*, **17**, 518 (1978); b) *idem, Chem. Lett.*, **1979**, 1251; c) *idem, Bull. Chem. Soc. Jpn.*, **54**, 473 (1981).
13) G. Yamamoto, *Tetrahedron*, **46**, 2761 (1990).
14) a) G. Yamamoto and M. Ōki, *Chem. Lett.*, **1979**, 1255; b) *idem, Bull. Chem. Soc. Jpn.*, **54**, 481 (1981).
15) A part of the results has been reported in preliminary forms: a) G. Yamamoto, *Chem. Lett.*, **1990**, 1373. b) *idem, Chem. Lett.*, **1991**, 741.
16) D. A. Kleier and G. Binsch, QCPE Program No. 165.
17) R. B. Nachbar, Jr. and K. Mislow, QCPE Program No. 559.
18) For the nomenclature of conformers, see: L. C. Closs and W. Klyne, *Pure Appl. Chem.*, **45**, 11 (1976).
19) L. Pauling, "The Nature of the Chemical Bond," 3rd ed, Cornell University Press, New York (1960), p. 260.
20) M. Nishio and M. Hirota, *Tetrahedron*, **45**, 7201 (1989); M. Ōki, *Acc. Chem. Res.*, **23**, 351 (1990).
21) *ap*-**7** and *sc1*-**7**: T. Nemoto, A. Uchida, Y. Ohashi, and G. Yamamoto, *Acta Crystallogr., Sect. C*, submitted; *ap*-**8** and *sc1*-**8**: T. Nemoto, T. Ono, A. Uchida, Y. Ohashi, and G. Yamamoto, *ibid.*, submitted.
22) G. Yamamoto and M. Ōki, *Bull. Chem. Soc. Jpn.*, **58**, 1953 (1985).
23) S. Gronowitz and G. Hansen, *Ark. Kemi*, **27**, 145 (1967).
24) G. Yamamoto and M. Ōki, *Bull. Chem. Soc. Jpn.*, **56**, 2082 (1983).